Currents through Hv1 channels deplete protons in their vicinity

Víctor De-la-Rosa, Esteban Suárez-Delgado, Gisela E. Rangel-Yescas, and León D. Islas

Departamento de Fisiología, Facultad de Medicina, Universidad Nacional Autónoma de México, México DF 04510, México

Proton channels have evolved to provide a pH regulatory mechanism, affording the extrusion of protons from the cytoplasm at all membrane potentials. Previous evidence has suggested that channel-mediated acid extrusion could significantly change the local concentration of protons in the vicinity of the channel. In this work, we directly measure the proton depletion caused by activation of Hv1 proton channels using patch-clamp fluorometry recordings from channels labeled with the Venus fluorescent protein at intracellular domains. The fluorescence of the Venus protein is very sensitive to pH, thus behaving as a genetically encoded sensor of local pH. Eliciting outward proton currents increases the fluorescence intensity of Venus. This dequenching is related to the magnitude of the current and not to channel gating and is dependent on the pH gradient. Our results provide direct evidence of local proton depletion caused by flux through the proton-selective channel.

The Journal of General Physiology

INTRODUCTION

Cells from different lineages possess proton currents with distinct physiological roles, varying from cytoplasmic pH regulation to specialized roles in the innate immune response (DeCoursey, 2013; Okamura et al., 2015). The physical identity of the channels mediating these currents was first revealed by the molecular cloning of the Hv1 and VSOP proton channels, which, unexpectedly, are formed by voltage-sensing domains possessing a proton-selective pathway (Ramsey et al., 2006; Sasaki et al., 2006).

Although the details of the proton transport mechanism are still not clear, it has been proposed that protons are carried by a diffusion-limited mechanism and that proton channels have a discrete conductance, similarly to other bona fide ion channels. A noise analysis study has reported estimates of the single-channel conductance of proton currents in eosinophils (Cherny et al., 2003). This conductance is very small, in the order of 140 fS at an intracellular pH (pH_i) of 5.5, partly because the proton concentration is very small. The single-channel conductance of the cloned Hv1 is unknown but assumed to be similarly small to that of native channels. In addition to being proton-permeable, hHv1 channels display a pH-dependent gating mechanism, in which the voltage dependence of channel opening is shifted to negative voltages when the proton gradient increases and favors outward proton flux. The mechanism of this pH dependence is unknown, but it ensures that protons are always transported outside of the cell upon hHv1 activation (Cherny et al., 1995).

Large changes in the local concentration of ions are expected in the vicinity of ion channels, especially when the equilibrium ionic concentrations are very asymmetric. This is the case of calcium (Ca^{2+}) ions and calcium channels, where the existence of microdomains with very high Ca^{2+} concentrations near the intracellular mouth of the ion channel have been well documented and even shown to have a functional role (Wagner and Keizer, 1994; Berridge, 2006). A similar but somewhat inverse situation is to be expected of protons. The cytoplasmic proton concentration under physiological conditions is in the order of 60 nM (approximate pH 7.2), so even small outward fluxes could significantly alter the local intracellular concentration of protons.

The physiological concentration of protons is very low; thus, previous work has attempted to determine whether the single-channel conductance of proton channels is limited by diffusion of the buffer to the entrance of the channel or by the rate of a protonation–deprotonation reaction at the intracellular entrance of the channel. Those experiments concluded that the rate-limiting step in conduction occurs in the permeation pathway (DeCoursey and Cherny, 1996). However, several other experiments have shown evidence of insufficient control of pH and proton depletion, indicating that buffer diffusion might play an important role in determining proton conduction (Kapus et al., 1993; Cherny et al., 2003). In this work, we provide direct evidence derived from fluorescence measurements in the immediate vicinity of the channel of a decreased availability of protons as a consequence of proton transport through Hv1 channels.

Correspondence to León D. Islas: lislas@canales.facmed.unam.mx

V. De-la-Rosa's present address is Dept. of Physiology and Biophysics, Virginia Commonwealth University, Richmond, VA 23298.

Abbreviations used in this paper: FP, fluorescent protein; GFP, green FP; pH_i, intracellular pH.

© 2016 De-la-Rosa et al. This article is distributed under the terms of an Attribution–Noncommercial–Share Alike–No Mirror Sites license for the first six months after the publication date (see http://www.rupress.org/terms). After six months it is available under a Creative Commons License (Attribution–Noncommercial–Share Alike 3.0 Unported license, as described at http://creativecommons.org/licenses/by-nc-sa/3.0/).

The Rockefeller University Press $30.00
J. Gen. Physiol. Vol. 147 No. 2 127–136
www.jgp.org/cgi/doi/10.1085/jgp.201511496

MATERIALS AND METHODS

Molecular biology and channel expression

The human proton channel hHv1 construct was a gift from I.S. Ramsey (Virginia Commonwealth University, Richmond, VA). This construct contains the Venus variant of green fluorescent protein (FP [GFP]) at the N terminus of the channel and is cloned into pcDNA6.2-DEST, and in this work it is referred to as Venus-Hv1. Using this construct, mutation H148G was inserted into Venus (VenusH148G-hHv1). An additional construct where Venus was placed at the end of the C terminus of hHv1 was made and termed Hv1-Venus. Other constructs were made based on Hv1-Venus. All C-terminal constructs have a GGGG linker between the end of the channel and the Venus FP. The mutant C-terminal −4 has a deletion of the sequence KTRS at the beginning of the C-terminal coiled-coil helices, whereas the C-terminal +4 mutant has the insertion of the sequence ERQL immediately after KTRS. Overlap PCR was used to make these mutant channels. Plasmids were linearized with the AgeI restriction enzyme, and mRNA was synthesized in vitro with the mMESSAGE mMACHINE T7 transcription kit (Ambion).

Xenopus laevis oocytes were surgically extracted and defolliculated as previously described (Ishida et al., 2015). Oocytes were incubated at 18°C in ND96 solution containing (mM) 96 NaCl, 2 KCl, 1.8 $CaCl_2$, 1 $MgCl_2$, 5 HEPES, 2.5 pyruvic acid, and 20 µg/ml gentamycin (pH 7.5, NaOH). Oocytes were injected with 40–50 nl of mRNA (∼1 µg/ml) at least 6 h after harvesting using a Manual Oocyte Microinjector (Drummond Scientific) and glass capillaries drawn to ∼20-µm-diameter opening. Experiments were performed 3–4 d after injection.

Patch-clamp fluorometry

hHv1-mediated proton currents were recorded in the inside-out patch-clamp configuration with an Axopatch 200B patch-clamp amplifier (Axon Instruments, Inc.). Data were recorded through an ITC-18 interface (InstruTech, Inc.) using the Pulse software package (HEKA). Analysis was performed with Pulse and Igor Pro software (WaveMetrics). Macroscopic currents were filtered at 2 kHz and sampled at 10 kHz. Patch pipettes had a resistance of ∼3 MΩ. Bath and pipette solutions contained (mM) 1 EGTA, 2 $MgCl_2$, 10 MES/HEPES, and 90 sucrose, and the pH was adjusted with NMDG.

Fluorescence images were recorded in a TE-2000U (Nikon) inverted epifluorescence microscope with a Luca EMCCD camera (Andor) while the proton current was simultaneously recorded. Fluorescence was acquired by imaging the patch pipette with a 60× oil immersion objective (numerical aperture 1.4; Nikon). The excitation light source was an Ar-Ion laser (Spectra-Physics). The laser was coupled to a single-mode optical fiber, collimated, and then focused into the objective back focal plane using optics mounted in an optical cage system (Thorlabs). An excitation filter selected the 488-nm laser line and fluorescence emission was filtered with a 530/10-nm band pass emission filter. Images were acquired and analyzed with Micro-Manager software and ImageJ (National Institutes of Health; Edelstein et al., 2010).

Membrane patches were held at −80 mV, the voltage was stepped to −100 mV for 1.2 s, and during this voltage step, fluorescence emission was acquired with a 300-ms exposure that ended ∼50 ms before the test pulse. Then the voltage was stepped from −100 to 100 mV in 20-mV steps for 1.2 s (test pulse) during which a second fluorescence image was captured with the same exposure (the last 300 ms of the test pulse); finally, the voltage was returned to −30 mV in some experiments or to −80 mV, as indicated in each figure. Currents were not corrected for linear leak and capacitive components. Proton currents, I_H, were converted to conductance, G_H, according to

$$I_H = G_H\left(V - V_H\right). \tag{1}$$

Here, V_H is the proton current reversal potential, given by the Nernst equation.

The voltage dependence of G_H was fitted to

$$G_H\left(V\right) = \frac{1}{1+\exp\left[q_a\left(V - V_{0.5}\right)/kT\right]}. \tag{2}$$

The parameter q_a is the apparent valence associated with gating, in elementary charge (e_o) units, and $V_{0.5}$ is the voltage of mid activation.

For image analysis, fluorescence intensity was measured from the whole patch or from a horseshoe-like region of interest (ROI) drawn around the patch dome with similar results. Change in fluorescence was calculated by dividing the intensity obtained at the test pulse by the intensity at −100 mV for the same sweep. Some pipettes exhibited areas of significant fluorescence outside of the patch area; because these membrane segments are not voltage-clamped, fluorescence from them was excluded from the measurements; nevertheless, this fluorescence serves as a negative control for the changes in fluorescence in the patch membrane. All images were background-subtracted using a region outside the pipette image as background.

Fluorescence imaging of membrane sheets

The vitelline membrane from *Xenopus* oocytes expressing Venus or VenusH148G-labeled channels was mechanically removed. These oocytes were then placed in a poly-D-lysine–coated glass coverslip, which also constituted the bottom of the chamber for fluorescence imaging. After 15–30 min, the oocyte was carefully removed from the chamber, leaving a small sheet of membrane attached to the glass (De-la-Rosa et al., 2013). Membrane sheets were washed with a solution of 500 mM NaCl to remove yolk vesicles, and the bathing solution was then changed to varying pH solutions ranging from 3 to 10, with the same composition as used for patch-clamp recording. Fluorescence appears spotty because of channel cluster formation. Mean emission intensity of a single spot or a large area of the membrane sheet was measured with identical results. Fluorescence intensity was normalized to the value at the highest pH. Results were fitted to a titration curve of the form

$$F = F_o + \frac{\left(1 - F_o\right)}{1 + 10^{\left(\mathrm{pK}_a - \mathrm{pH}\right)}}, \tag{3}$$

where F_o is the residual fluorescence at low pH and pK_a is the pH at which $F = (1 + F_o)/2$.

Online supplemental material

Supplemental material is included in the form of one figure (Fig. S1) that contains the mean conductance versus voltage curves of Hv1-Venus channels obtained at two different pH gradients used in these experiments. Online supplemental material is available at http://www.jgp.org/cgi/content/full/jgp.201511496/DC1.

RESULTS

Given the very small concentration of protons in the cytoplasm, it has been suggested that as protons permeate through proton channels, the local proton concentration would be altered. Indirect evidence for this can be seen in the current "droop" or apparent inactivation that is produced when large proton currents are achieved

(DeCoursey and Cherny, 1996). Given that this depletion could potentially produce significant changes in local pH, we reasoned that a pH-sensitive FP attached to the channel could behave as a local pH reporter.

The GFP is highly sensitive to pH, losing fluorescence intensity when its fluorophore becomes protonated. This is the reason why GFP and other variants of it have been used as indicators of cellular and organellar bulk pH (Bizzarri et al., 2009).

Fig. 1 A shows patch-clamp fluorometry recordings of the fluorescence of Hv1 channels that have been tagged with the Venus FP in the N terminus. Venus is a variant of the yellow FP (YFP) that has increased brightness and retains pH sensitivity (Nagai et al., 2002). These recordings were performed at a nominal pH_i of 5.5 in the presence of 100 mM MES buffer. The fluorescence of channels in the patch could be readily detected and proton currents recorded simultaneously. As the depolarizing pulse was made more positive, outward currents were elicited, and in fact, at very positive potentials there was a time-dependent decrease of the current magnitude, which has been taken as an indication of permeant ion depletion (Fig. 1 B).

Measurement of the patch fluorescence near the end of the depolarizing pulse showed that its magnitude increased, relative to the fluorescence at a negative potential (Fig. 1 D). The magnitude of the fluorescence increase can be superimposed on the current to voltage relationship (I-V curve), indicating that fluorescence is a function of current magnitude, even at voltages where channel activation, measured by the conductance calculated according to Eq. 1, reaches saturation (Fig. 1, C and D). It should be noted that because of proton depletion, the G-V curve is underestimated, but it should still provide an estimate of Hv1 channel gating. One possible explanation for the increase in fluorescence is

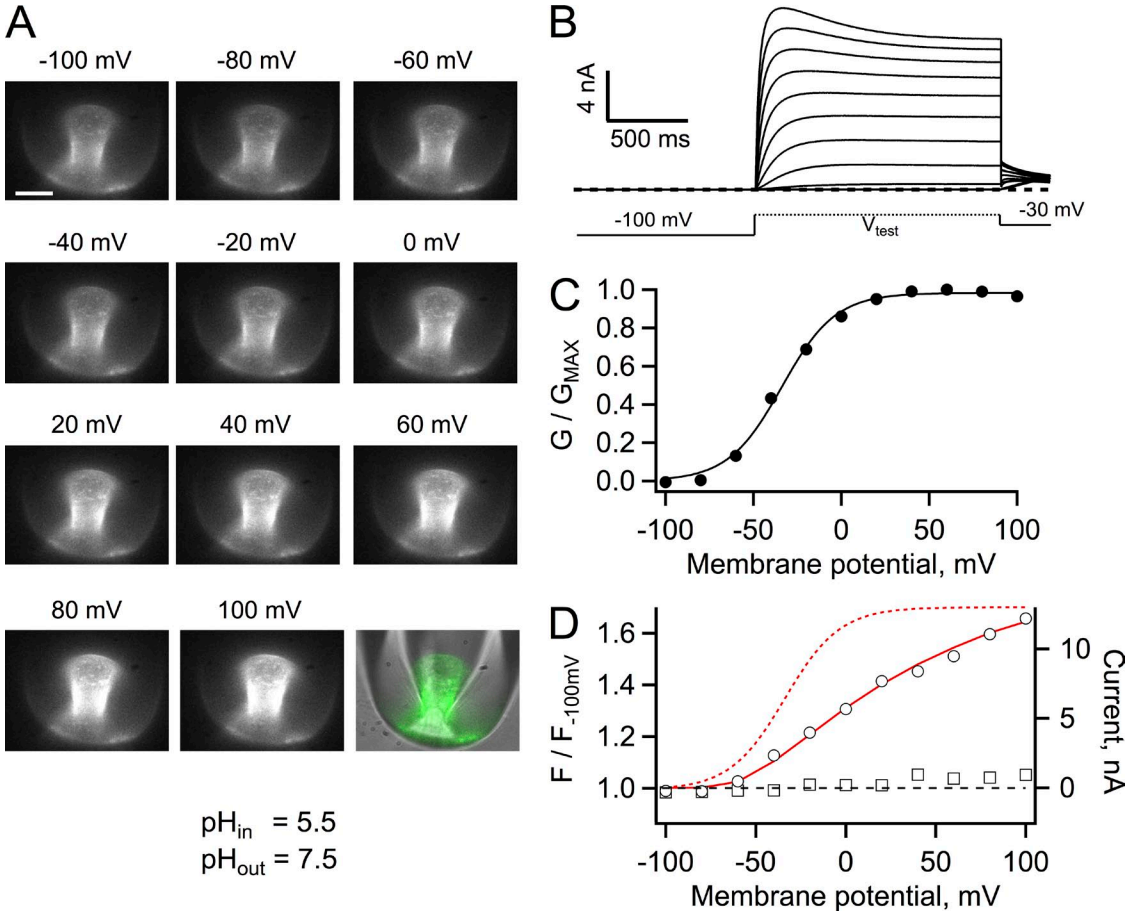

Figure 1. Patch-clamp fluorometry of Venus-Hv1. (A) Fluorescence images of an inside-out patch held at the indicated membrane potential. The image in the bottom right corner is a superposition of the fluorescence image at 100 mV (green) and the transmitted light image of the pipette to show the location of the membrane patch within the pipette. Bar, 10 µm. (B) Proton currents from the patch in A elicited by depolarizing voltage-clamp pulses. (C) Conductance versus voltage curve derived from the currents in B. The continuous line is a fit to Eq. 2 with parameters $q_a = 1.63\ e_o$ and $V_{0.5} = -33.8$ mV. (D) Fluorescence measured from the whole patch area at each voltage was normalized to the fluorescence at −100 mV (circles). A ratio greater than one indicates an increase (dequenching) of the fluorescence. The fluorescence of a region of membrane attached to the pipette but outside of the patch is also plotted (squares). The red continuous line is the I-V curve from the currents in A, whereas the red dashed curve is the fit to the G-V curve in C. The bath solution contained 100 mM MES buffer, and the pH of solutions is indicated.

that the FP could be tracking activation of Hv1, as in other engineered fluorescent voltage sensors (Baker et al., 2012; Mutoh et al., 2012). This explanation is unlikely because the fluorescence signal is related to the magnitude of the current and not to channel gating (Fig. 1, C and D). Moreover, the magnitude of the fluorescence change is very large and represents an increase of fluorescence, which is opposite to the small amplitude quenching that is observed in most fluorescent voltage sensors based on a single FP.

The patch in Fig. 1 had exceptionally large currents. More typical currents were <1,000 pA at 80 mV, and under these conditions fluorescence dequenching in 100 mM buffer, although present, was difficult to quantify. We decided to carry out the rest of the experiments in the presence of 10 mM buffer, still a condition with very high buffering power. Experiments with the more typical current magnitudes gave the same qualitative result (Fig. 2).

Fig. 2 shows that the same fluorescence dequenching behavior could be observed if the FP was placed in the C or N terminus of hHv1. As for the data in Fig. 1, the fluorescence follows the I-V curve and not the G-V curve, again indicating that it is related to proton permeation and not channel gating. In these particular patches, the magnitude of fluorescence dequenching was smaller than in Fig. 1, in accordance with the smaller current magnitude as can be seen from the value of the currents in the superimposed I-V curves. These data show that the fluorescence in a single patch follows the increase in current regardless of the position of the FP. The crystal structure of the C terminus of VSOP extends beyond the cytoplasmic side of the membrane by ∼80 Å (Fujiwara et al., 2012; Fujiwara and Okamura, 2014), and the fusion of the FP should add ∼30 Å. Increasing or decreasing this distance by 4 aa, ∼10 Å, did not produce noticeably different fluorescence increases as a function of current (see Fig. 4), indicating that the proton depletion zone extends beyond 10 nm into the cytoplasm (Fujiwara et al., 2012).

The pK_a of the fluorescence of Venus is 5.73 (see Fig. 5 and Nagai et al. [2002]), so if the fluorescence increase was indeed related to proton depletion and not to a voltage-dependent process, it would be expected that at a higher pH_i the fluorophore in Venus would be deprotonated and its fluorescence would be independent of current. Fig. 3 shows that at pH_i 7 proton currents

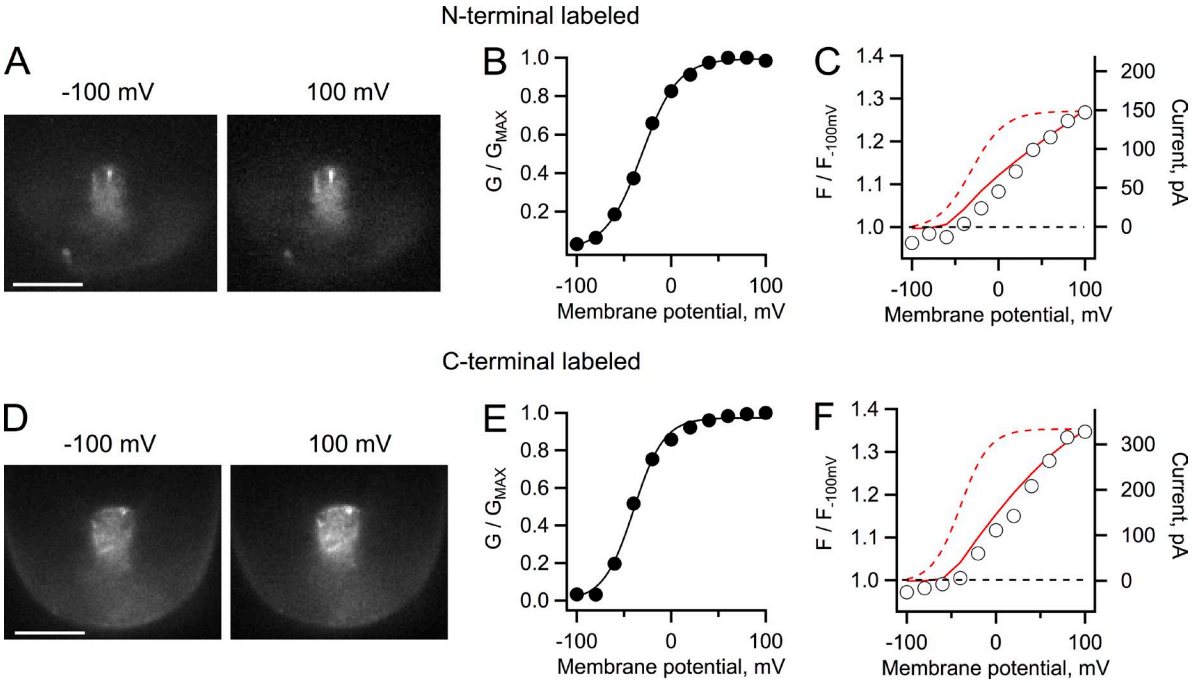

Figure 2. Patch-clamp fluorometry of Venus-Hv1 and Hv1-Venus constructs. (A) Fluorescence images of an inside-out patch from an oocyte expressing Hv1 channels labeled with Venus in the N terminus. The patch was held at the indicated membrane potential. (B) G-V curve from proton currents from the patch in A elicited by depolarizing voltage-clamp pulses. The continuous line is a fit to Eq. 2 with parameters q_a = 1.31 e_o and $V_{0.5}$ = −31.2 mV. (C) Fluorescence measured from the whole area of the patch in A at each voltage, plotted as normalized intensity with respect to the fluorescence intensity at −100 mV. (D) Fluorescence images from an inside-out patch from oocytes expressing the Hv1 construct labeled at the C terminus. (A and D) Bars, 10 µm. (E) G-V curve from proton currents from the same patch in D elicited by depolarizing voltage-clamp pulses. The continuous line is a fit to Eq. 2 with parameters q_a = 1.56 e_o and $V_{0.5}$ = −39.6 mV. (F) Fluorescence measured from the whole patch area and analyzed as in C. For the analysis in C and F, a ratio greater than one indicates an increase (dequenching) of the fluorescence as the patch is held at increased positive potentials. The red continuous line is the I-V curve from the currents in the corresponding patch, whereas the dashed curve is the fit to the G-V curve. The buffer concentration for these experiments was 10 mM MES, and the pH gradient is as in Fig. 1.

activated at higher potentials and with slower kinetics, as expected from the pH dependence of Hv1 gating (Fig. 3, B and C; and Fig. S1). In this recording condition, even though proton currents should be producing proton depletion, the fluorescence no longer increased as a function of current (Fig. 3 D), presumably because at pH 7 Venus is completely deprotonated and its fluorescence is no longer sensitive to pH. This result provided further evidence that the fluorescence change is related to the proton current magnitude.

The data presented in Figs. 1, 2, and 3 can be explained if the outward proton flux produced a local pH_i increase in the periphery of the Venus FP, leading to dequenching of the fluorescence.

In Fig. 4, the magnitude of the fluorescence increase was plotted as a function of the size of the proton current at the same voltage of 80 mV for a series of different patches and constructs. The data show that there is a nonlinear correlation between the two quantities. Because even at pH_i 5.5 the proton concentration is only 3.16 µM, the proton current I_H is sustained by the flux of protonated buffer. A previous study (Cherny et al., 2003) developed a quantitative treatment of the expected proton depletion effects caused by proton fluxes. The theoretical results in that work predict that the local proton concentration should be a function of channel current amplitude, just as our experimental observation. We have combined their equation A12, which relates the proton concentration to the proton current, with the titration curve expected for a FP to give an equation relating fluorescence to proton current amplitude:

$$F = \frac{1}{1+10^{fpK_a-pH}}$$

and

$$pH = -\log\left\{K_a\left(\frac{1-\alpha_o-\beta_i I_H}{\alpha_o+\beta_i I_H}\right)\right\}. \quad (4)$$

In these equations, fpK_a is the pK_a of the FP, K_a is the buffer dissociation constant, α_o is the degree of buffer dissociation, I_H is the magnitude of the proton current, and β_i is a factor that takes into account the dimensions of the patch pipette under the supposition that the patch can be represented as a truncated cone:

$$\beta_i = \frac{1}{\pi b F D_{BH} B_{total}}\left(\frac{1}{r_o}-\frac{1}{r_p}\right)$$

with

$$b = \frac{r_p - r_o}{l_p}.$$

Here, F is Faraday's constant, D_{BH} is the buffer diffusion coefficient, B_{total} is the total concentration of buffer, and

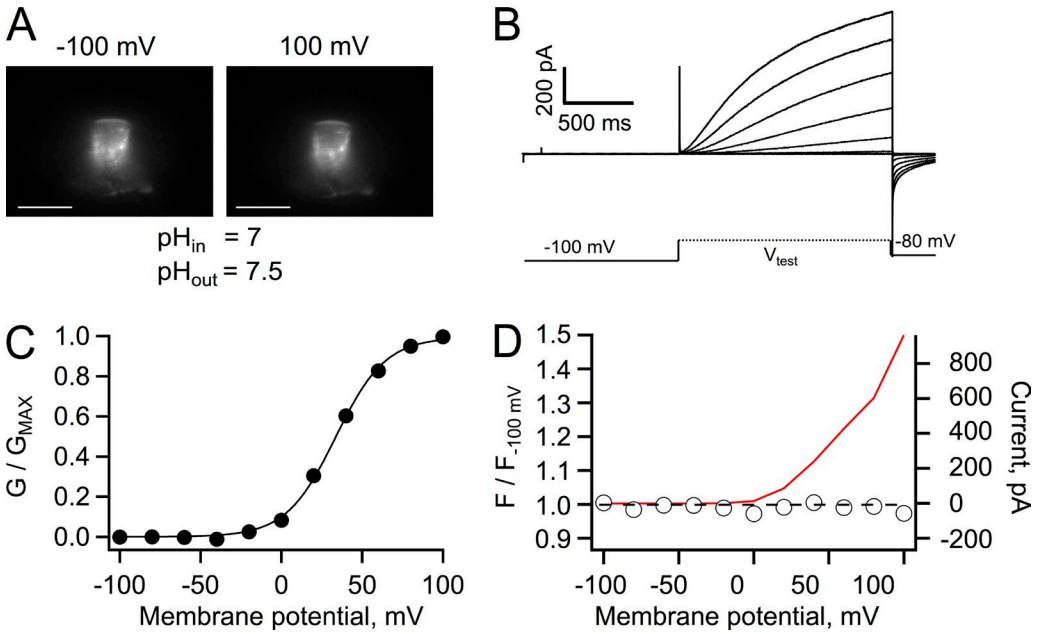

Figure 3. Patch-clamp fluorometry of Venus-Hv1 at pH_i 7. (A) Fluorescence images of an inside-out patch held at the indicated membrane potential. Bars, 10 µm. (B) Proton currents from the patch in A elicited by depolarizing voltage-clamp pulses, as indicated by the schematic protocol. (C) Conductance versus voltage curve derived from the currents in B. The continuous line is a fit to Eq. 2 with parameters $q_a = 1.62\ e_o$ and $V_{0.5} = 33.6$ mV. (D) Fluorescence measured from the whole patch area at each voltage was normalized to the fluorescence at −100 mV. A ratio equal to one at all voltages indicates the absence of dequenching of the fluorescence of Venus. The red continuous line is the I-V curve from the currents in B. The bath solution contained 10 mM HEPES buffer.

r_o, r_p, and l_p are the radius of pipette opening, radius of the patch, and the length of the patch, respectively. These factors can readily be estimated from our fluorescence patch images (Fig. 4 A). The continuous line in Fig. 4 B is the predicted magnitude of the fluorescence dequenching as a function of proton current amplitude (Eq. 4), calculated for the recording conditions of pH_i 5.5, K_a for MES, and α_o for MES at pH 5.5. The used pK_a is that of Venus. The agreement between the experimental data and the theoretical expectation strongly suggests that the increased fluorescence signal is reporting on increased local pH at the FP.

An immediate prediction of the data in Figs. 3 and 4 is that if the FP had a higher pK_a, we should recover the increase in fluorescence even at pH_i 7. To test this hypothesis, we sought to change the pK_a of Venus by introducing a mutation at position H148. This amino acid has been shown to influence the pK_a of GFP-related proteins profoundly (Wachter et al., 1998; Hanson et al., 2002). The mutation H148G shifted the pK_a of Venus from 5.73 to 7.62, as estimated by titrating the fluorescence of membrane sheets prepared from oocytes expressing the corresponding Venus fused to the N terminus of Hv1 (Fig. 5). When currents and fluorescence from the construct VenusH148G-Hv1 were recorded at pH_i 7, we recovered the fluorescence increase. Importantly, fluorescence dequenching now occurred at more positive potentials and overlapped

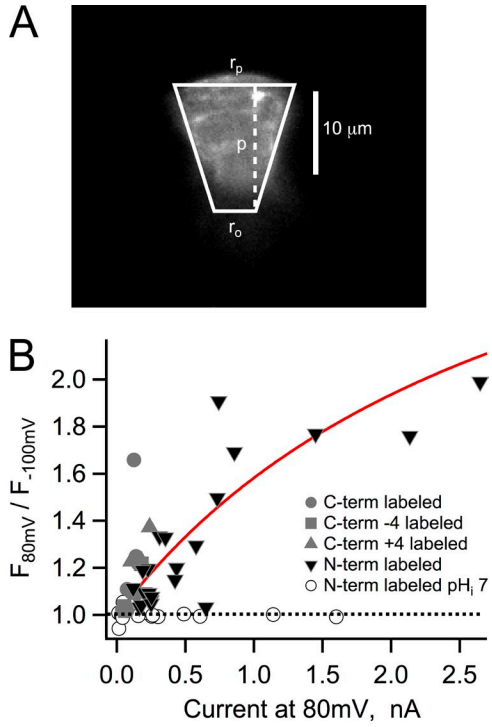

Figure 4. Fluorescence dequenching and proton depletion. (A) Fluorescence image of a typical patch expressing Hv1-Venus and approximation of its geometry by a truncated cone with the indicated dimensions used in the model in Eq. 4. (B) The value of the observed dequenching at 80 mV is plotted as a function of the current for that particular patch also at 80 mV. All of the experiments in this figure were obtained with an intracellular solution of pH 5.5, with the exception of those patches represented by the open circles. The continuous red curve is the dequenching as a function of current magnitude predicted by Eq. 4. The parameters that went into Eq. 4 were r_p = 10 µm, r_o = 5 µm, l_p = 15 µm, $K_a = 7.08 \times 10^{-7}$, α_o = 0.1812, fpK_a = 5.6, $D_{BH} = 5 \times 10^{-10}$ m^2/s, and B_{total} = 10 mM. The dotted line indicates lack of dequenching and describes the recordings from N-labeled channels at pH_i 7.

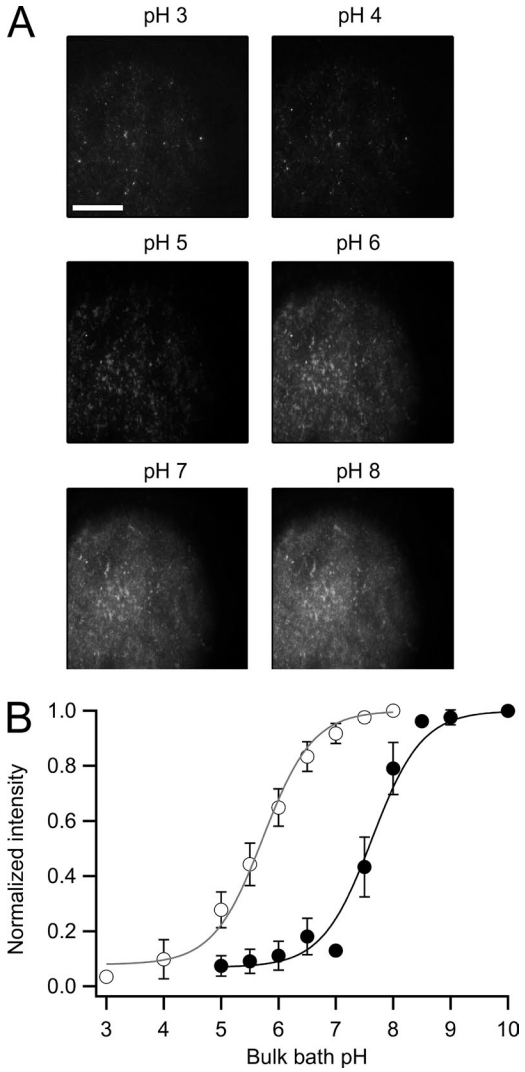

Figure 5. Measurement of the pK_a of fluorescent constructs. (A) Representative membrane sheet from oocytes injected with the Venus-Hv1 construct. The membrane was imaged under different pH conditions, indicated at the top of each frame. Fluorescence was measured as the mean of an ROI encompassing a large area of the membrane sheet or from individual clusters of channels with the same results. Bar, 20 µm (same for all images). (B) The fluorescence was normalized to the value at the highest pH for each construct to build the full titration curve. The data were fitted to the titration function (Eq. 3). The pK_a for Venus-Hv1 (open circles) is 5.63 and 7.62 for VenusH148G-Hv1 (closed circles). The data are the mean of five experiments for both constructs, and error bars are the standard error of the mean.

the development of outward proton current, as expected from the positively shifted voltage dependence at symmetrical pH (Fig. 6 D). Data from several patches again showed the correlation between dequenching and current magnitude, confirming that the local pH_i is being increased by the proton flux. It should be noted that the fluorescence increase was smaller in magnitude than that observed at pH_i 5.5 (Fig. 4), in part because of the reduced concentration of protons at pH_i 7 and the smaller expression level of the construct VenusH148G-Hv1. Still, the data can be explained by the dequenching model embodied in Eq. 4 (Fig. 6 E).

DISCUSSION

Local proton depletion produced by activation of Hv1 channels is to be expected as part of their function. Simultaneous recordings of pH_i and proton current activation have been performed in the past in intact cells and have shown that whole-cell proton flux in small cells is enough to alkalinize the bulk cytoplasm by about +1 pH unit (Thomas and Meech, 1982; Kapus et al., 1993). Here we show that, remarkably, even in an inside-out patch where the buffer is available in essentially infinite supply (with respect to the proton flux), a proton current can locally deplete hydronium ions by a large amount.

In analogy with Ca^{2+} ion concentration microdomains (Berridge, 2006), the existence of pH microdomains around proton channels might play a functionally important role, especially if pH-sensitive proteins associate with proton channels or are localized in their immediate vicinity.

Even though our fluorescence measurements are not absolutely calibrated as a function of pH, we can estimate the change in pH from the titration curves of the fluorescent chimeric channels (Fig. 5). From these data, it can be expected that the fluorescence of the VenusHv1 construct at pH 5.5 would be quenched by 56%. Thus, the observed increase of 60% in the fluorescence at 80 mV, as in Fig. 1 D, represents a change of 1 pH unit. Even when current magnitude is <20 times that in Fig. 1, dequenching at maximum conductance (80 mV) can be >40%, which translates into an alkalinization of just under a pH unit.

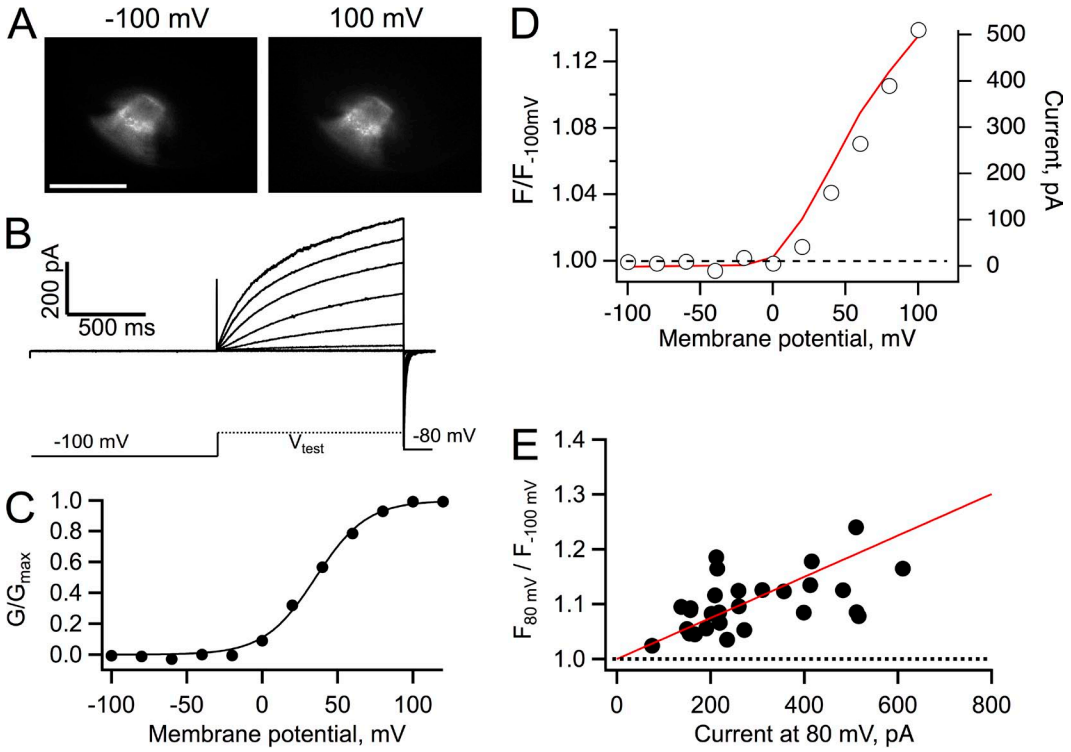

Figure 6. Recovery of fluorescence dequenching in VenusH148G-Hv1 at pH_i 7. (A) Fluorescence images of an inside-out patch from an oocyte expressing the construct VenusH148G-Hv1 held at the indicated membrane potential. Bar, 10 µm. (B) Proton currents from the patch in A elicited by depolarizing voltage-clamp pulses. (C) Conductance versus voltage curve derived from the currents in B. The continuous line is a fit to Eq. 2 with parameters $q_a = 1.47\ e_o$ and $V_{0.5} = 35.4$ mV. (D) Fluorescence dequenching measured from the whole area of the patch in A. The red curve is the I-V curve for the same patch. (E) The fluorescence from 28 patches similar to A was measured at 80 mV, normalized to the fluorescence at −100 mV, and plotted as a function of the current magnitude at 80 mV, as in Fig. 4. A ratio greater than one at all voltages indicates dequenching of the fluorescence of VenusH148G. The bath solution contained 10 mM HEPES buffer. The continuous red line is the predicted dequenching by Eq. 4 with parameters $r_p = 10$ µm, $r_o = 5$ µm, $l_p = 15$ µm, $K_a = 2.81 \times 10^{-8}$, $\alpha_o = 0.26$, $fpK_a = 7.6$, $D_{BH} = 5 \times 10^{-10}$ m^2/s, and $B_{total} = 10$ mM.

Cherny et al. (2003), assuming that the main limitation to proton conductance is buffer diffusion and deprotonation, provided a quantitative description of proton depletion at the channel entrance. We have used this as the basis for a description of the effect of local proton depletion on the fluorescence reported by Venus. This model can reasonably account for the data, but some assumptions need commenting. Eq. 4 supposes a conical geometry for the patch, and our images can be well approximated by this geometry, thus allowing for a direct estimation of the model parameters related to patch shape. However, the prediction in Fig. 4 B assumes a mean patch, so the scatter of the data might result from the different sizes and relative parameters of the membrane patches involved in the analysis in Fig. 4.

Why is the proton depletion effect so marked in Hv1 channels? An initial simple model for depletion is to consider a proton channel as a point sink for protons (Fig. 7 A). If the outward proton current, I_H, is given by q, the proton concentration c, considering only radial diffusion in the r direction, is given by the solution to the diffusion equation with appropriate boundary and initial conditions (Crank, 1979):

$$c(r,t) = c_\infty - \frac{q}{2\pi D_H r}\left(erfc\left(\frac{r}{2\sqrt{D_H t}}\right)\right),$$

where D_H is the diffusion coefficient of protons in water and c_∞ is the bulk proton concentration.

In the steady state, this equation simplifies to

$$c(r) = c_\infty - \frac{q}{2\pi D_H r}. \tag{5}$$

This function is plotted in Fig. 7 B for different values of the bulk concentration and the same value of q and D_H. If the value of c_∞ is large, in the millimolar to high micromolar range, the flux q is not enough to reduce the proton concentration significantly from its bulk value, until r is smaller than an angstrom; however, for values of c_∞ in

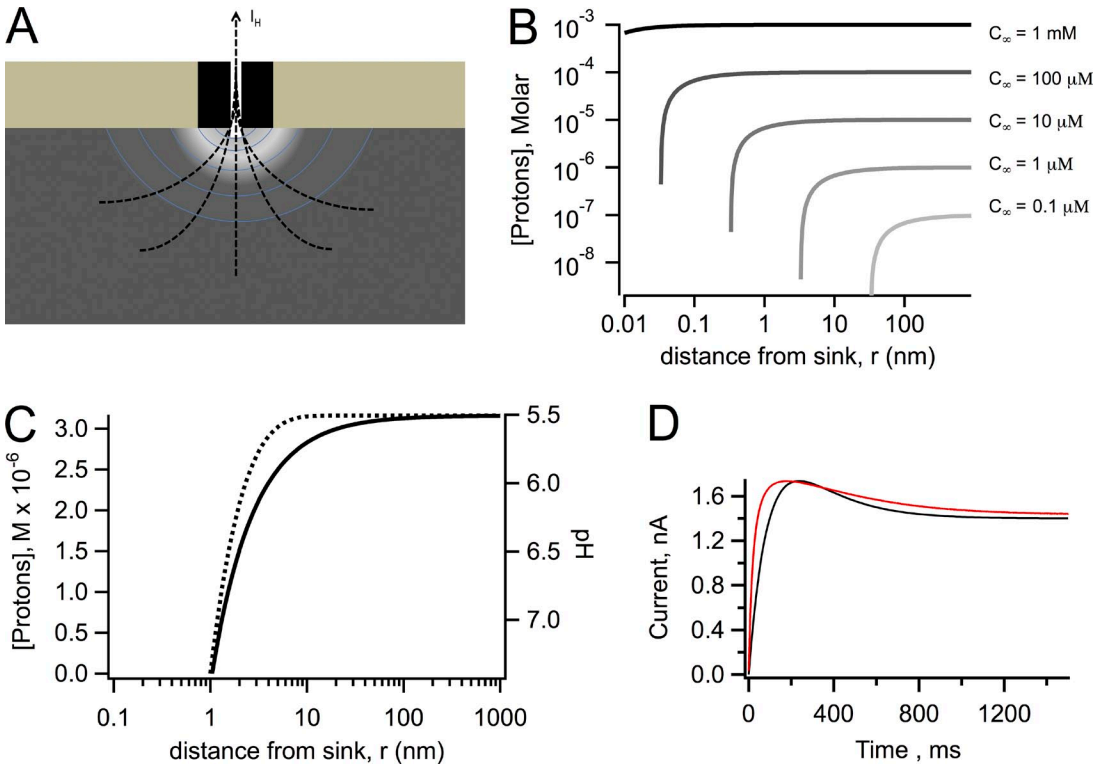

Figure 7. Diffusion model calculations. (A) Schematic representation of the proton depletion zone generated by an outward proton current through an Hv1 channel. (B) Calculations using Eq. 5 of the extent of the depletion of protons as a function of the radial coordinate, r, for different values of the bulk proton concentration, c_∞, as indicated; the value of q = 14 fA is the same for all curves as well as D_H = 7,000 µm^2/s. (C) Calculation of the effect of the presence of buffer. The black curve was calculated with D_H = 7,000 µm^2/s and Eq. 5. The effect of the presence of buffer is illustrated by the dotted line, which was calculated with Eq. 6. The values of the constants are c_∞ = 3.16 µM, [B] = 100 mM, a = 1 nm, $k_b = 10^{10}$ M^{-1}s^{-1}, and D_H = 7,000 µm^2/s. Data are presented as molar proton concentration (left axis) and corresponding pH (right axis). (D) Experimental (red) and simulated (black) currents in response to a 100-mV depolarization. Simulated current trace was generated taking into account a pH change during current development of 1 pH unit, which changes the single-channel current from 5 fA to 1.4 fA. The current is given by Eq. 7 in the form $I(H,t) = N \bullet \left(1 - e^{-t/\tau}\right)\left[5 - (5 - 1.4)\left(1 - e^{-t/\tau}\right)\right]$, with τ = 200 ms and N as an arbitrary whole number chosen to match the size of the experimental current.

the low micromolar range, the flux can significantly reduce the concentration even at distances greater than several tens of angstroms from the sink, creating a depletion microdomain around the proton channel pore.

The presence of buffers does not make the depletion effect disappear. A simple model of proton diffusion in the presence of a rapidly equilibrating buffer has been proposed in Decker and Levitt (1988) and Nunogaki and Kasai (1988). The solution for the proton concentration $c(r)$ profile in the presence of a rapid buffer is given by

$$c(r) = c_\infty \left(1 - (a/r)\mathrm{e}^{-\lambda(r-a)}\right),$$

with

$$\lambda^2 = k_b [B] / D_H, \quad (6)$$

where $[B]$ is the concentration of buffer, k_b is the association rate constant, and a is the capture radius of the channel pore. This function also predicts a large depletion of protons in the vicinity of a proton channel, although it happens over a narrower range of values of r (Fig. 7 C).

In our experiments with patches with very large currents and in published whole-cell recordings also with large proton fluxes (Kapus et al., 1993; DeCoursey and Cherny, 1996; Iovannisci et al., 2010), it is observed that the time course of proton current shows an apparent inactivation phenomenon, which is not present in smaller currents or currents recorded in the absence of a pH gradient. Similar apparent inactivation phenomena have been observed in CNG channels and are caused by permeant ion depletion and accumulation (Zimmerman et al., 1988). To what extent can our estimates of local proton changes explain the kinetics of the apparent inactivation? Noise analysis experiments in native proton currents (Cherny et al., 2003) have estimated the dependence of the single-channel proton current, i_s, on intracellular proton concentration. They report that for a 1 pH unit decrease, i_s increases approximately four times; so for the 1 pH change from 5.5 to ~6.5 estimated for the data in Fig. 1, i_s goes from ~5 fA to ~1.4 fA. A simple model of the macroscopic proton current is given by

$$I_H(t,H) = N \bullet P_o(t) \bullet i_s(t,H). \quad (7)$$

Assuming first-order kinetics for P_o and a time course for the change in i_s with the same kinetics as P_o, the calculated time course of current at 100 mV ($P_o \sim 1$) using Eq. 7 is very similar to the experimental time course with the pseudo-inactivation (Fig. 7 D), strongly suggesting that the estimated pH change around the channel can qualitatively explain the altered kinetics.

Our findings confirm that even in the presence of a large buffering power, proton currents significantly deplete protons in the vicinity of the channel and alter pH, even in inside-out patch recording conditions, so that the concentration of protons near the channel is not well controlled, when the total membrane proton current is too large. Proton channels have very small single-channel conductance but still are capable of playing a role in pH_i regulation. This is possible in part because the intracellular proton concentration is very small, thus even small fluxes can easily change pH, and in part because the cell must be able to insert a high number of channel molecules in the membrane to ensure sufficient proton flux. Finally, our data show that currently, Hv1 channels cannot be used as the basis for fluorescent membrane potential sensors, unless truly pH-insensitive FPs are used. In contrast, constructs such as the one used here could be used in conjunction with bulk cytoplasmic pH sensors to study pH dynamics in different regions of the cell.

The authors would like to thank Dr. T. Rosenbaum for helpful discussions.

This work was supported by grant no. IN209515 from DGAPA-PAPIIT-UNAM.

The authors declare no competing financial interests.

Sharona E. Gordon served as editor.

Submitted: 11 August 2015
Accepted: 21 December 2015

REFERENCES

Baker, B.J., L. Jin, Z. Han, L.B. Cohen, M. Popovic, J. Platisa, and V. Pieribone. 2012. Genetically encoded fluorescent voltage sensors using the voltage-sensing domain of *Nematostella* and *Danio* phosphatases exhibit fast kinetics. *J. Neurosci. Methods.* 208:190–196. http://dx.doi.org/10.1016/j.jneumeth.2012.05.016

Berridge, M.J. 2006. Calcium microdomains: organization and function. *Cell Calcium.* 40:405–412. http://dx.doi.org/10.1016/j.ceca.2006.09.002

Bizzarri, R., M. Serresi, S. Luin, and F. Beltram. 2009. Green fluorescent protein based pH indicators for in vivo use: a review. *Anal. Bioanal. Chem.* 393:1107–1122. http://dx.doi.org/10.1007/s00216-008-2515-9

Cherny, V.V., V.S. Markin, and T.E. DeCoursey. 1995. The voltage-activated hydrogen ion conductance in rat alveolar epithelial cells is determined by the pH gradient. *J. Gen. Physiol.* 105:861–896. http://dx.doi.org/10.1085/jgp.105.6.861

Cherny, V.V., R. Murphy, V. Sokolov, R.A. Levis, and T.E. DeCoursey. 2003. Properties of single voltage-gated proton channels in human eosinophils estimated by noise analysis and by direct measurement. *J. Gen. Physiol.* 121:615–628. http://dx.doi.org/10.1085/jgp.200308813

Crank, J. 1979. The Mathematics of Diffusion. Second edition. Oxford University Press, New York. 414 pp.

De-la-Rosa, V., G.E. Rangel-Yescas, E. Ladrón-de-Guevara, T. Rosenbaum, and L.D. Islas. 2013. Coarse architecture of the transient receptor potential vanilloid 1 (TRPV1) ion channel determined by fluorescence resonance energy transfer. *J. Biol. Chem.* 288:29506–29517. http://dx.doi.org/10.1074/jbc.M113.479618

Decker, E.R., and D.G. Levitt. 1988. Use of weak acids to determine the bulk diffusion limitation of H+ ion conductance through the gramicidin channel. *Biophys. J.* 53:25–32. http://dx.doi.org/10.1016/S0006-3495(88)83062-5

DeCoursey, T.E. 2013. Voltage-gated proton channels: molecular biology, physiology, and pathophysiology of the H_V family. *Physiol. Rev.* 93:599–652. http://dx.doi.org/10.1152/physrev.00011.2012

DeCoursey, T.E., and V.V. Cherny. 1996. Effects of buffer concentration on voltage-gated H+ currents: does diffusion limit the conductance? *Biophys. J.* 71:182–193. http://dx.doi.org/10.1016/S0006-3495(96)79215-9

Edelstein, A., N. Amodaj, K. Hoover, R. Vale, and N. Stuurman. 2010. Computer control of microscopes using μManager. *Curr. Protoc. Mol. Biol.* Chapter 14:20.

Fujiwara, Y., and Y. Okamura. 2014. Temperature-sensitive gating of voltage-gated proton channels. *Curr. Top. Membr.* 74:259–292. http://dx.doi.org/10.1016/B978-0-12-800181-3.00010-5

Fujiwara, Y., T. Kurokawa, K. Takeshita, M. Kobayashi, Y. Okochi, A. Nakagawa, and Y. Okamura. 2012. The cytoplasmic coiled-coil mediates cooperative gating temperature sensitivity in the voltage-gated H^+ channel Hv1. *Nat. Commun.* 3:816. http://dx.doi.org/10.1038/ncomms1823

Hanson, G.T., T.B. McAnaney, E.S. Park, M.E. Rendell, D.K. Yarbrough, S. Chu, L. Xi, S.G. Boxer, M.H. Montrose, and S.J. Remington. 2002. Green fluorescent protein variants as ratiometric dual emission pH sensors. 1. Structural characterization and preliminary application. *Biochemistry.* 41:15477–15488. http://dx.doi.org/10.1021/bi026609p

Iovannisci, D., B. Illek, and H. Fischer. 2010. Function of the HVCN1 proton channel in airway epithelia and a naturally occurring mutation, M91T. *J. Gen. Physiol.* 136:35–46. http://dx.doi.org/10.1085/jgp.200910379

Ishida, I.G., G.E. Rangel-Yescas, J. Carrasco-Zanini, and L.D. Islas. 2015. Voltage-dependent gating and gating charge measurements in the Kv1.2 potassium channel. *J. Gen. Physiol.* 145:345–358. http://dx.doi.org/10.1085/jgp.201411300

Kapus, A., R. Romanek, A.Y. Qu, O.D. Rotstein, and S. Grinstein. 1993. A pH-sensitive and voltage-dependent proton conductance in the plasma membrane of macrophages. *J. Gen. Physiol.* 102:729–760. http://dx.doi.org/10.1085/jgp.102.4.729

Mutoh, H., W. Akemann, and T. Knöpfel. 2012. Genetically engineered fluorescent voltage reporters. *ACS Chem. Neurosci.* 3:585–592. http://dx.doi.org/10.1021/cn300041b

Nagai, T., K. Ibata, E.S. Park, M. Kubota, K. Mikoshiba, and A. Miyawaki. 2002. A variant of yellow fluorescent protein with fast and efficient maturation for cell-biological applications. *Nat. Biotechnol.* 20:87–90. http://dx.doi.org/10.1038/nbt0102-87

Nunogaki, K., and M. Kasai. 1988. The H^+/OH^- flux localizes around the channel mouth in buffered solution. *J. Theor. Biol.* 134:403–415. http://dx.doi.org/10.1016/S0022-5193(88)80070-5

Okamura, Y., Y. Fujiwara, and S. Sakata. 2015. Gating mechanisms of voltage-gated proton channels. *Annu. Rev. Biochem.* 84:685–709. http://dx.doi.org/10.1146/annurev-biochem-060614-034307

Ramsey, I.S., M.M. Moran, J.A. Chong, and D.E. Clapham. 2006. A voltage-gated proton-selective channel lacking the pore domain. *Nature.* 440:1213–1216. http://dx.doi.org/10.1038/nature04700

Sasaki, M., M. Takagi, and Y. Okamura. 2006. A voltage sensor-domain protein is a voltage-gated proton channel. *Science.* 312:589–592. http://dx.doi.org/10.1126/science.1122352

Thomas, R.C., and R.W. Meech. 1982. Hydrogen ion currents and intracellular pH in depolarized voltage-clamped snail neurones. *Nature.* 299:826–828. http://dx.doi.org/10.1038/299826a0

Wachter, R.M., M.A. Elsliger, K. Kallio, G.T. Hanson, and S.J. Remington. 1998. Structural basis of spectral shifts in the yellow-emission variants of green fluorescent protein. *Structure.* 6:1267–1277. http://dx.doi.org/10.1016/S0969-2126(98)00127-0

Wagner, J., and J. Keizer. 1994. Effects of rapid buffers on Ca2+ diffusion and Ca2+ oscillations. *Biophys. J.* 67:447–456. http://dx.doi.org/10.1016/S0006-3495(94)80500-4

Zimmerman, A.L., J.W. Karpen, and D.A. Baylor. 1988. Hindered diffusion in excised membrane patches from retinal rod outer segments. *Biophys. J.* 54:351–355. http://dx.doi.org/10.1016/S0006-3495(88)82966-7